Determining the material structure of microcrystalline silicon from Raman spectra

C. Smit[a)]
Eindhoven University of Technology, Department of Applied Physics, P. O. Box 513, 5600 MB Eindhoven, The Netherlands

R. A. C. M. M. van Swaaij[b)]
Delft University of Technology, DIMES-ECTM, P. O. Box 5053, 2600 GB Delft, The Netherlands

H. Donker
Delft University of Technology, Laboratory for Inorganic Chemistry, Julianalaan 136, 2628 BL Delft, The Netherlands

A. M. H. N. Petit
Delft University of Technology, DIMES-ECTM, P. O. Box 5053, 2600 GB Delft, The Netherlands

W. M. M. Kessels and M. C. M. van de Sanden
Eindhoven University of Technology, Department of Applied Physics, P. O. Box 513, 5600 MB Eindhoven, The Netherlands

(Received 25 October 2002; accepted 10 June 2003)

An easy and reliable method to extract the crystalline fractions in microcrystalline films is proposed. The method is shown to overcome, in a natural way, the inconsistencies that arise from the regular peak fitting routines. We subtract a scaled Raman spectrum that was obtained from an amorphous silicon film from the Raman spectrum of the microcrystalline silicon film. This subtraction leaves us with the Raman spectrum of the crystalline part of the microcrystalline film and the crystalline fraction can be determined. We apply this method to a series of samples covering the transition regime from amorphous to microcrystalline silicon. The crystalline fractions show good agreement with x-ray diffraction (XRD) results, in contrast to crystalline fractions obtained by the fitting of Gaussian line profiles applied to the same Raman spectra. The spectral line shape of the crystalline contribution to the Raman spectrum shows a clear asymmetry, an observation in agreement with model calculations reported previously. The varying width of this asymmetrical peak is shown to correlate with the mean crystallite size as determined from XRD spectra. [DOI: 10.1063/1.1596364]

I. INTRODUCTION

Hydrogenated amorphous silicon (*a*-Si:H) has been studied for application in solar cells for several decades. Nowadays, microcrystalline silicon (μc-Si:H) also receives much attention because it is a suitable material for application as the intrinsic layer in the bottom cell of thin-film tandem solar cells. To study the material properties, the complete set of analysis techniques used in *a*-Si:H research (reflection/transmission spectroscopy, subgap absorption, dark and photoconductivity, etc.) can be copied, although carefully.[1] In addition, the study of this material should also include the determination of the crystalline fraction, because μc-Si:H silicon is a heterogeneous material and consists of crystalline and amorphous regions. The fraction of crystalline material, the crystallite size, and the grain boundaries have an important influence on the optical and electrical properties that are relevant for application in solar cells. Void and grain boundaries, for example, could contain a high density of recombination centers, whereas a high crystalline fraction is likely to increase the mobility of the charge carriers.

Four techniques are commonly used to analyze the structural properties of μc-Si:H: high-resolution transmission electron microscopy (HRTEM), x-ray diffraction (XRD), spectroscopic ellipsometry (SE), and Raman spectroscopy. However, none of these techniques leads to an unambiguous determination of the crystalline fraction in μc-Si:H films. First, HRTEM is a complicated technique and its respective images have a poor contrast on amorphous material, so regions where amorphous and crystalline material overlap in the sample will appear to be fully crystalline in the two-dimensional image. Therefore, it is difficult to determine the crystalline fraction in microcrystalline material from these images, unless the crystalline fraction is so small (smaller than a few percent) that the crystals do not overlap in the image. Particle sizes, though, can be extracted. Second, XRD is an easier technique, but a reasonable scan takes at least 2 h for films of about 500 nm thick. Also, it is not straightforward to extract the crystalline fraction, although some researchers reported doing so.[2,3] The average particle size can be extracted from the XRD peak widths. Third, SE is a

[a)]Also at: Delft University of Technology, DIMES-ECTM, P. O. Box 5053, 2600 GB Delft, The Netherlands.
[b)]Author to whom correspondence should be addressed; electronic mail: r.vanswaaij@dimes.tudelft.nl

simple and easy measurement technique. It gives the dielectrical constant as a function of energy, which is fitted with a model containing parameters like film thickness and crystalline and void fractions.[4] However, it is not unambiguous as to which model is accurate and realistic.

A fourth technique to analyze the structural properties is Raman spectroscopy. Most methods used in literature to obtain crystalline fractions from Raman spectra are based on peak fitting and suffer from interpretation problems. For example, often, three peaks instead of two (one for the crystalline and one for amorphous part) are necessary to fit the experimental data. The need for three peaks is often explained by introducing an extra phase in the material. Furthermore, the crystalline fractions that result from peak fitting are very sensitive to the choice of input parameters, like whether peak positions are allowed to vary and the range of data points that is included in the fitting procedure.

In this article, we will first review reported methods to obtain information on the material structure from Raman spectra. Then, we propose an alternative approach to separate the amorphous and the crystalline contributions to the Raman spectrum of the microcrystalline silicon film that is to be examined. This method is applied to a series of silicon films that covers the transition from amorphous to microcrystalline. We will show that this technique automatically resolves several problems related to the methods used in literature. Finally, we shall compare crystalline fractions obtained with this method with results from XRD analysis and Gaussian line profile fitting procedures on the same samples and present our conclusions.

II. RAMAN SPECTRUM OF MICROCRYSTALLINE SILICON

A. The Raman spectrum

In a solid, a small part of the energy of an incoming photon can be used to excite a lattice vibration (phonon). The remaining energy escapes as a photon with a slightly smaller energy compared to the incoming photon. This energy shift is denoted as a Raman shift. In a crystalline solid, the momentum conservation law selects only phonons with zero momentum, because the momentum of the photon is negligibly small. In monocrystalline silicon, only the optical phonon with energy 64 meV has zero momentum and this leads to the sharp peak at a Raman shift of $520\,\mathrm{cm}^{-1}$ [Fig. 1(a)]. In *a*-Si:H, the momentum selection rule is relaxed and a variety of phonon modes and energies are allowed.[5] A broad peak centered at $480\,\mathrm{cm}^{-1}$ now dominates the Raman spectrum [Fig. 1(b)]. μc-Si:H can be considered as a mix of crystalline Si (*c*-Si) and *a*-Si:H. The Raman spectrum, however, is not simply the sum of a monocrystalline silicon and an amorphous silicon spectrum, as can be seen in Fig. 1(c). This is due to the fact that the Raman spectrum of a small crystallite is different from a Raman spectrum of monocrystalline silicon. It is not straightforward how to determine which part of the spectrum is due to the crystalline fraction and which part can be attributed to the amorphous fraction in μc-Si:H. This determination is necessary, though, in order to extract the crystalline fraction from Raman spectra.

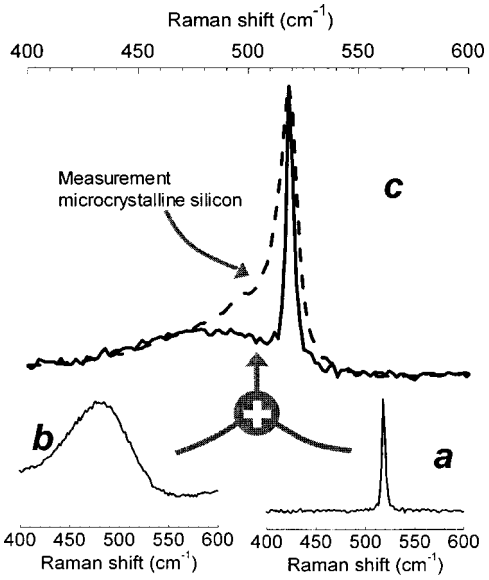

FIG. 1. (a) Raman spectrum of monocrystalline silicon. (b) Raman spectrum of *a*-Si:H. (c) Summation of (a) and (b) (solid line), scaled before summation by the eye so that the peak and the "bump" in (c) fit the peak and the "tail" of the Raman spectrum of μc-Si:H (dashed line).

B. Ways to get the material structure from Raman spectroscopy

We will first shortly review several techniques that have been reported to separate the Raman spectra into a crystalline and an amorphous contribution. The simplest way is just to compare the peak height at $520\,\mathrm{cm}^{-1}$ to the peak height at $480\,\mathrm{cm}^{-1}$ (e.g., see Ref. 6). This comparison gives only a very rough estimate of the crystallinity of the material. Peak fitting is more frequently used to unravel the spectrum. For example, two peaks (Gaussian or Lorentzian line profiles) can be used, one to describe the crystalline part and one for the amorphous part, but this procedure does not lead to a good fit to the measured Raman spectrum. Furthermore, the low-energy peak, which is attributed to the amorphous fraction, tends to shift to higher energies than the expected $480\,\mathrm{cm}^{-1}$. As we will show later, this shift is not due to a shift of the amorphous transverse optical (TO) phonon energy, but to the change in the Raman peak shape of the crystalline fraction. In order to obtain a good fit to the measured spectra, at least three peaks are necessary.[2,7] The third peak is then attributed to surface modes[7] or to hexagonal ordered silicon.[2]

The peak fitting routines described herein require this extra peak because the peak shape of the crystalline part is asymmetric and varies for different samples. As calculated by Richter *et al.*[5] and Campbell *et al.*,[8] the crystalline peak width and position is influenced by the crystallite size and shape. For example, calculations show that this peak becomes more and more asymmetric for smaller crystallite sizes. Touir *et al.*[9] account for this by using two asymmetrical Lorentzian line profiles to obtain a good fit to their spectra. They find peaks around $500\,\mathrm{cm}^{-1}$ and $520\,\mathrm{cm}^{-1}$ (and so do we with our samples as we will show in Sec. IV D), which they attribute to two distinct crystallite sizes. How-

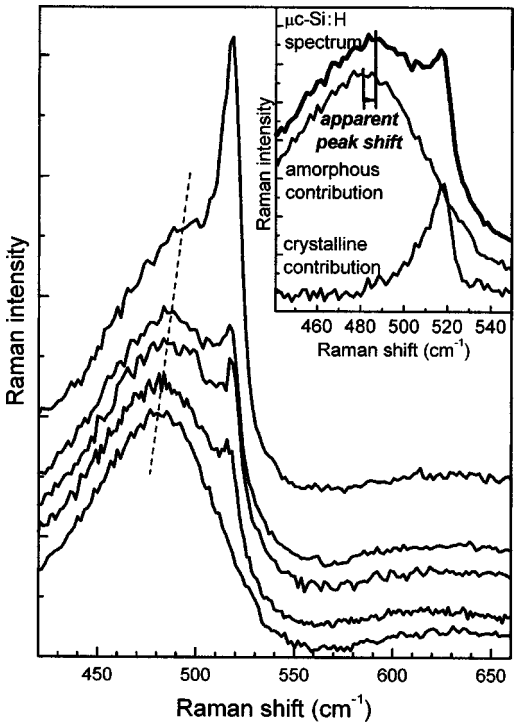

FIG. 2. The amorphous peak of the Raman spectrum of μc-Si:H seems to shift to higher energies with increasing crystalline fraction. Inset: The amorphous contribution plus the crystalline contribution make the microcrystalline spectrum. The addition of the sloped shoulder of the crystalline contribution seems to shift the maximum in the spectrum of the amorphous sample to a higher energy in the spectrum of the microcrystalline sample. This shift could abusively be interpreted as a shift of the amorphous TO phonon energy.

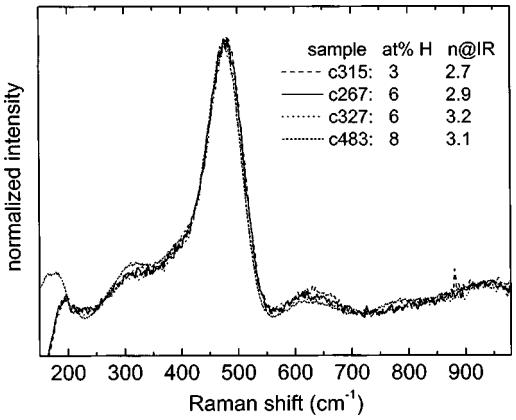

FIG. 3. Raman spectra of four *a*-Si:H films with varying refractive index and hydrogen content.

ever, the idea of two crystallite sizes is not attractive, because a continuous distribution of sizes seems more likely. Furthermore, only the TO phonon mode of *a*-Si:H is included in the fitting procedures mentioned herein, while the amorphous longitudinal optical (LO) phonon mode, and maybe even the Si–H wagging mode at 660 cm^{-1} and the transverse acoustic (TA) phonon mode of the amorphous fraction, have an influence on the microcrystalline Raman spectrum in the energy region of the crystalline feature (around 520 cm^{-1}). In addition, the amorphous peak in the Raman spectrum of μc-Si:H has been reported to shift to higher energy with increasing crystalline fraction. This shift is attributed to an extra TO band at about 490 cm^{-1}, indicating a secondary phase in the amorphous material.[10] We also observe this apparent peak shift (Fig. 2).

In contrast to the Raman signal of the small crystallites in μc-Si:H, the Raman signal of *a*-Si:H is shown to vary only slightly between different samples. Spectra taken from some of our own amorphous samples deposited under different processing conditions show no significant differences for the range investigated (Fig. 3). In line with this result, Ishidate *et al.*[11] found TO phonon energy shifts of only a few cm^{-1} and peak width variations of a few percent at most when the hydrogen content is varied from 6 to 18 at. %. This strongly suggests that the Raman spectrum of the amorphous fraction in μc-Si:H can be represented by the Raman spectrum of *a*-Si:H. Therefore, it must be possible just to subtract the amorphous contribution to the Raman spectrum of μc-Si:H with the help of a Raman spectrum of an amorphous film. The advantage is that in the unravelling of the Raman spectrum of μc-Si:H, not only the TO phonon mode of the amorphous component, is taken into account but also the other phonon modes. After the substraction, changes in the peak shape of the crystalline contribution to the Raman spectrum of μc-Si:H become clearly visible. The apparent peak shift shown in Fig. 2 can now be explained in a natural way as illustrated in the inset of Fig. 2: When the TO phonon peak in the Raman spectrum of an *a*-Si:H film is added to the asymmetrical sloped shoulder of the Raman peak of the crystalline fraction in μc-Si:H, then the position of the peak in the resulting line shape is expected to shift.

III. EXPERIMENT

We deposited two series of silicon films of about 600 nm thick on Corning glass C1737 and [100] oriented, slightly *n*-type, *c*-Si substrates simultaneously, using expanding thermal plasma chemical vapor deposition.[12] Details on the deposition setup are reported elsewhere.[13] The first series of samples is deposited using an Ar flow of 1200 sccm, a H_2 flow of 600 sccm, and a varying SiH_4 flow from 0.5 to 10 sccm. The second series is deposited using a constant SiH_4 flow of 5 sccm and a varying hydrogen flow. The argon flow was set at twice the hydrogen flow. A third series of samples is deposited using a pure H_2 plasma with a H_2 flow of 2000 sccm and a varying SiH_4 flow on glass and Al foil and the films are about 5000 nm thick.

The Raman spectra of the silicon films on the glass substrates are measured using a Raman microscope (Renishaw-(Gloucestershire, UK) Ramascope system 2000, grating 1800 lines/mm) in a backscattering geometry with a 2 mW Ar laser at a wavelength of 514.5 nm focused in a spot of about 1 μm. On the samples on *c*-Si substrates of the third sample series, one XRD measurement is carried out (Bruker–Nonius (Delft, The Netherlands) D5005 θ/θ diffractometer with diffracted beam graphite monochromator, wavelength Cu α). On these samples three with Al substrates, XRD measurements are also carried out to determine the crystalline fraction.

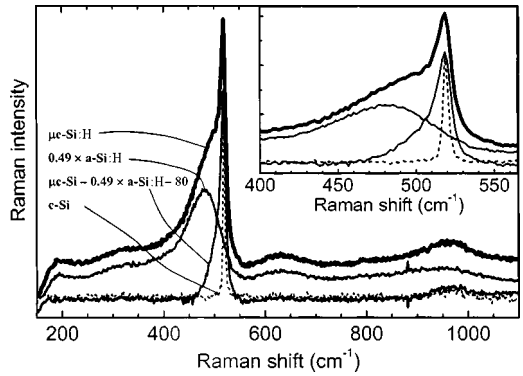

FIG. 4. From a Raman spectrum of μc-Si:H (thick line), a Raman spectrum of *a*-Si:H (thin line) is subtracted to obtain the contribution of the crystalline fraction. The scaling factor for the amorphous contribution and the flat background are obtained in a least-squares procedure. For comparison, the Raman spectrum of monocrystalline silicon is shown also (dashed line). The inset contains a magnification of the TO phonon peak region.

IV. RESULTS AND DISCUSSION

A. Splitting a Raman spectrum into a crystalline and an amorphous contribution

In order to split the Raman spectrum of a μc-Si:H film into a crystalline and an amorphous contribution, we subtract a scaled Raman spectrum of an *a*-Si:H film (Fig. 4). The result is denoted as μc-Si:H$-A\times a$-Si:H$-$B, where *B* is a flat background to correct for the dark counts and background light. Because of differences in signal strength (caused by differences in sample alignment and film composition) the amorphous spectrum is scaled by factor *A* before subtraction. The values for this constant and background are obtained in a least-squares routine, realizing that the crystalline contribution to the spectrum of μc-Si:H cannot contain peaks at the amorphous acoustical phonon energies. That means that the residue in the regions in the spectrum outside the TO phonon peak (we take the region 200 cm^{-1} to 440 cm^{-1} and 560 cm^{-1} to 850 cm^{-1}) should be minimized.

The resulting crystalline part of the spectrum shows a flat background, as can be seen in Fig. 4. The features at the low-energy side of the TO crystalline peak at 520 cm^{-1} in the amorphous and in the microcrystalline spectra (in the energy range of 150 cm^{-1} to 480 cm^{-1}) that are attributed to the LA, TA, and LO amorphous phonon modes are absent. Moreover, the broad features at the high-energy side in the amorphous and microcrystalline spectra at about 650 cm^{-1} and 950 cm^{-1}, which are attributed to two-phonon excitations in *a*-Si:H and to the Si–H wagging mode, are also subtracted correctly. The only feature that remains is a bump at 960 cm^{-1}. This feature is due to the two-phonon excitation process in *c*-Si (it can also be noticed in the Raman spectrum of μc-Si:H in Fig. 4) and should therefore be present in the Raman spectrum of the crystalline fraction. These observations strongly suggest that the procedure followed splits the Raman spectrum of μc-Si:H into the amorphous and the crystalline contributions. The small uncorrelated residue that is obtained after the subtraction is strong evidence for the assumption that the shape of the Raman spectrum of *a*-Si:H used in this procedure is the same as the shape of the Raman spectrum of the amorphous fraction in μc-Si:H.

B. Raman spectrum of the crystalline fraction

In Fig. 5, the XRD measurements of the first sample series (see Sec. III) are presented and it can be concluded that the samples deposited with SiH_4 flows from 0.5 to 5 sccm contain a crystalline fraction and the sample deposited with a SiH_4 flow of 10 sccm does not. The Raman spectra of the silicon films are split into an amorphous and a crystalline contribution following the procedure just described. The crystalline part of the Raman spectra is shown in Fig. 6. The spectra are normalized to the maximum of the Raman peak. For comparison, the Raman spectrum of μc-Si:H is also shown in Fig. 6. Clearly, the peak of the crystalline fraction in μc-Si:H is broader than the monocrystalline peak. It also clearly shows an asymmetry. Richter *et al.*[5] calculated the Raman spectrum of a finite-sized spherical silicon crystal and found a similar asymmetry. With smaller particle size, the momentum selection rule of the Raman process is more relaxed. With increasing momentum, the TO phonon energy becomes lower, so when a momentum greater than zero is

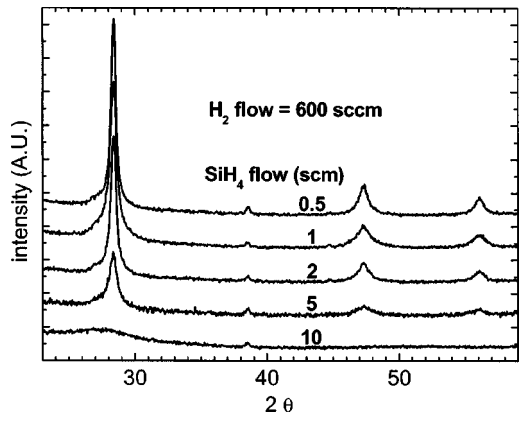

FIG. 5. XRD measurements of a series of samples deposited using a varying SiH_4 flow. Samples deposited using a SiH_4 flow up to 5 sccm show crystallinity.

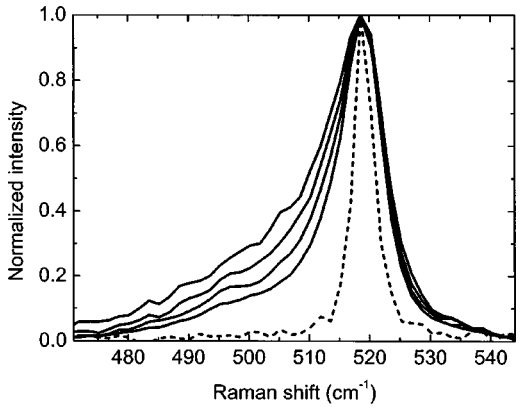

FIG. 6. The contributions of the crystalline fraction to the microcrystalline Raman spectrum normalized to one. Going from the narrow to the wide peak, the corresponding films are deposited using a SiH_4 flow of 0.5, 1, 2, and 5 sccm. The dashed line is the Raman spectrum of μc-Si:H.

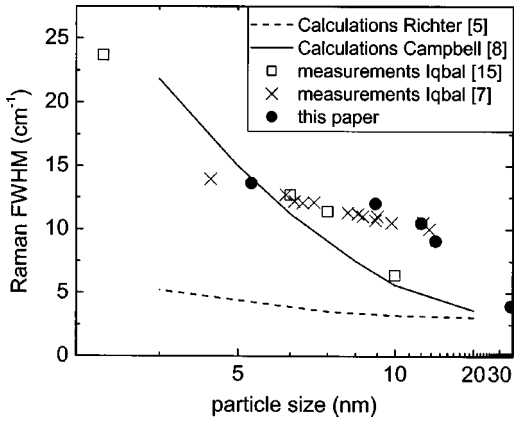

FIG. 7. The FWHM is displayed versus the average particle size as obtained from XRD measurements. Also, other reported data, experimental as well as calculated, are presented for comparison. The data point completely on the right-hand side of the reciprocal *x* axis is measured on an "infinitely" large *c*-Si wafer.

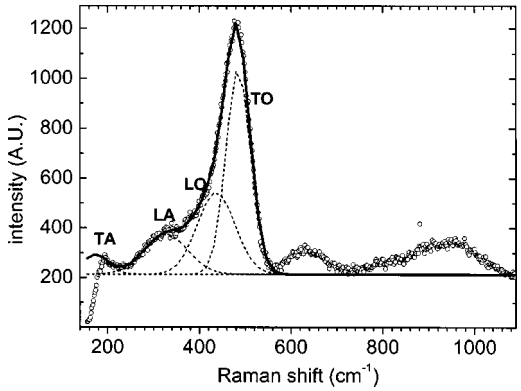

FIG. 8. Four Gaussian line profiles (dashed lines) are fitted to a Raman spectrum of *a*-Si:H to obtain the contribution of the TA, LA, LO, and TO phonon modes. The peak area of the TO phonon is used in the calculation of the amorphous fraction in the microcrystalline films.

allowed, lower-energy phonons will be excited. This leads to a broadening of the Raman peak toward the low-energy side, resulting in an asymmetrical peak shape.

The calculations of Richter *et al.*[5] explain the asymmetry, and revealed that the broadening depends on crystallite size. Figure 6 shows that the broadening increases with increasing silane flow. The average particle size is determined from the XRD measurements by applying the Scherrer equation to the integral width of the peak that corresponds to the reflection on the [220] lattice planes.[14] In Fig. 7, the average particle size is plotted against the full width of the Raman peak at half maximum, which shows a clear correlation. These data are in close agreement with measurements by Iqbal *et al.*,[7,15] although they use the full width half maximum (FWHM) of a fitted symmetrical Lorentzian line shape. Calculations of Campbell *et al.*[8] show a similar trend. It should be realized that the calculations concern Raman scattering on a ball-shaped particle having a specific size, while a distribution of particle sizes, maybe with different shapes, contributes to the experimental data. Also, calculated data of Richter *et al.*[5] are shown, but they show a large deviation from the other data in Fig. 7.

C. Determining the crystalline fraction

The peak areas of the crystalline and the amorphous parts of the Raman spectra correlate to the amount of *c*-Si and *a*-Si:H in the film. It is not possible to obtain absolute values because the detection efficiency is usually not known. The ratio of the two peak areas, however, corresponds to the ratio of the amount of crystalline to the amount of amorphous silicon. This ratio needs to be corrected for the difference in the cross sections for phonon excitation of *c*-Si compared to that of *a*-Si:H. For the TO phonon, the ratio of these two cross sections ($\sigma_{c\text{-Si}}/\sigma_{a\text{-Si:H}}$) is usually set at 0.8.[16,17] It should be noted that this cross section ratio is reported to depend on the crystallite size, and varies from about 0.9 to about 0.7 as the crystallite size ranges from 5 to 15 nm,[18] which are typical sizes for our samples. Now, we have to determine which part of the amorphous spectrum that is subtracted is due to the TO phonon excitation. In Fig. 8, the contributions of the four phonon modes are fitted to the amorphous spectrum using four Gaussian line profiles and the peak area of the TO phonon Raman scattering is determined. This number is multiplied by 0.8 to account for the cross section ratio and then multiplied by the scaling factor that is found from the least-squares procedure described herein to account for the amount of amorphous silicon in the microcrystalline film. The crystalline contribution is obtained by integrating the crystalline peak from $440\,\mathrm{cm}^{-1}$ to $560\,\mathrm{cm}^{-1}$. Following this procedure, the crystalline fractions were extracted from the Raman spectra of the samples of the second sample series. The result is shown in Fig. 9. At a SiH_4 dilution in H_2 of about 1%, the material changes from amorphous to microcrystalline. It can be noticed that the crystalline fraction saturates at a value a little below 0.8. This might be due to the grain boundaries, which can be considered as disordered material. However, it is reported that in fully nanocrystallized (free of amorphous material) silicon films (crystallite size around 5 nm), the amorphous Raman signal relative to the integral Raman signal from $440\,\mathrm{cm}^{-1}$ to $550\,\mathrm{cm}^{-1}$ amounts to less than 0.1.[19] This indicates that grain boundaries do not necessarily result in a saturation of the crystalline fraction at 0.8. It is, therefore, very possible

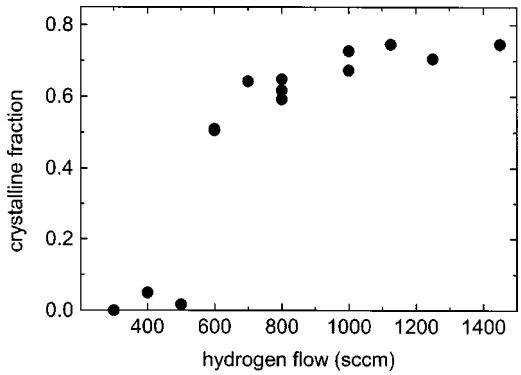

FIG. 9. The crystalline fraction versus the hydrogen flow used during deposition.

TABLE I. Crystalline fraction (%) determined from XRD and from Raman spectra using different techniques. The crystalline fractions determined from the Raman spectra are calculated using [cryst]/([cryst]+0.8*[am]) . First column: Silane flow. Second column: Crystalline fractions from XRD. Third column: Crystalline fraction determined as described in this article. Fourth column: For [cryst] and [am], the Raman intensities at $520\,cm^{-1}$ and $480\,cm^{-1}$, respectively, are taken. Fifth column: Fitting of three Gaussian line profiles as described in Refs. 2 and 20. Sixth column: Fitting of five Gaussian line profiles as described in Refs. 10 and 21. From a sample deposited with a silane flow of 18 sccm, no crystalline fraction was detected with all techniques.

SiH_4 flow (sccm)	XRD[a]	Raman	Raman [480] versus [520][b]	Raman (3 Gauss)	Raman (5 Gauss)
10	58±9	52±4	72±4	46±10	38±6
14	50±6	46±4	69±3	40±17	31±6
16	12±2	11±4	46±2	3±1.5	5.3±2.5

Note: cryst indicates crystalline and am indicates amorphous.
[a]See Ref. 3.
[b]See Ref. 6.

that a minimum of 10% to 20% of the amorphous material is characteristic for the deposition conditions used in this article.

D. Comparison with other techniques

To validate the method described herein to obtain crystalline fractions, the crystalline fractions of the third series of samples (see Sec. III) are determined from XRD measurements, using the method described by Williamson.[3] Furthermore, to compare our method with methods based on peak fitting, we also determined the crystalline fractions of these samples from the Raman spectra using techniques that are presented in literature. The results are shown in Table 1. In the second column, the crystalline fractions calculated from XRD measurements are shown. The third column contains the crystalline fractions determined from Raman spectra using the method presented in this article. In the fourth column, only the signal intensities at $480\,cm^{-1}$ and $520\,cm^{-1}$ are taken for the amorphous and the crystalline fraction respectively; a method used, for example, in Ref. 6. In the following column, the result from fitting three Gaussian line profiles is shown (fitting procedure is copied from Ref. 2),[20] followed by a fit procedure (copied from Ref. 10) using five Gaussian line profiles.[21] In Fig. 10, some of the fits are shown. Figures 10(a) and 10(b) show fits of three and five Gaussian line profiles, respectively. The asymmetrical peak of the crystalline fraction is approximated by two Gaussian line profiles on the high-energy side of the spectrum. At the lower-energies, peaks are fitted that represent the amorphous fraction. In Fig. 10(c), two asymmetrical Lorentzian line profiles are fitted to the spectrum, as reported by Touir *et al.*[9] A good fit to the data is obtained, but no amorphous peak is fitted and, therefore, the crystalline fraction cannot be calculated.

It should be mentioned that the calculated crystalline fractions are sensitive to the range of data that is fitted. For example, when the Raman spectrum deposited using 10 sccm of SiH_4 is fitted with three Gaussian line profiles (column 5, first row in Table 1) in the data range from $450\,cm^{-1}$ to $555\,cm^{-1}$ instead of $400\,cm^{-1}$ to $555\,cm^{-1}$, the crystalline fraction changes from 0.46 to 0.40. The errors in the crystalline fractions that are obtained by fitting Gaussian line profiles are calculated from the inaccuracies in the peak areas that originate from the fitting procedure. The errors in column 4 correspond to the error in the number of counts. The errors in the fractions that are obtained with the method presented in this article (column 3) are estimated from the noise in the background after the subtraction of the amorphous signal. As stated in Sec. IV (C) the ratio of the Raman scattering cross sections in *a*-Si:H and *c*-Si is set at 0.8 throughout this article, but can vary from 0.7 to 0.9 for the crystallite sizes in our samples.[18] This uncertainty results in an error of about 10% in the lower crystalline fractions and about 5% in the higher crystalline fractions. This error is neglected because it is smaller than the error induced by the noise in the measurements.

The crystalline fractions obtained by the method presented in this article are in good agreement with the XRD

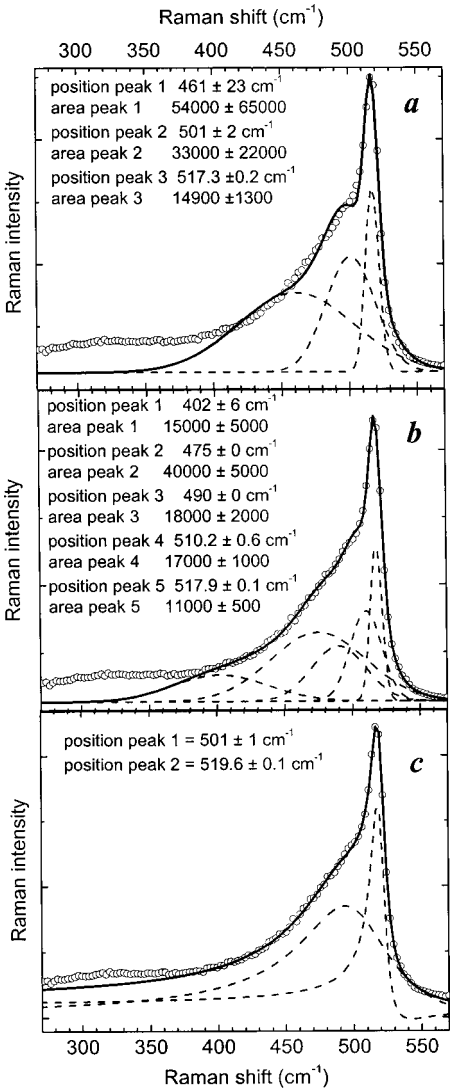

FIG. 10. Several fitting techniques that are described in literature, applied to a typical Raman spectrum of microcrystalline silicon. (a) Three Gaussian line profiles (see Refs. 2 and 20), (b) Five Gaussian line profiles (see Refs. 10 and 21), and (c) Two asymmetrical Lorentzian line profiles (see Ref. 9).

results. Crystalline fractions obtained with peak fitting techniques that are presented in literature do not agree as well with the XRD results. The method presented here is not sensitive to the range of data points that is included. Furthermore, it is straightforward what part should be attributed to the crystalline, and what part to the amorphous part of the spectrum. And finally, there is no discussion about peak positions that should be fixed or not to obtain realistic results. These are clear advantages above peak fitting methods. The earlier reported discrepancy (Refs. 2 and 22) in the crystalline fractions obtained from XRD and Raman spectroscopy is not observed in our samples when the subtraction method described in this article is applied to the Raman spectra.

V. CONCLUSION

We have demonstrated an alternative technique to extract the structural composition of μc-Si:H from Raman spectroscopy. Crystalline fractions obtained using this technique show good agreement with fractions obtained from XRD analysis, in contrast to crystalline fractions obtained by frequently used fitting procedures in literature. Furthermore, the subtraction of the amorphous part of the spectrum (taken from a Raman spectrum of an *a*-Si:H film) clearly reveals the asymmetrical peak shape of the Raman spectrum of the crystalline fraction as calculated in literature. Interpretation difficulties arising from peak fitting are resolved in a natural way.

ACKNOWLEDGMENTS

Professor D. L. Williamson (Colorado School of Mines) is gratefully acknowledged for the XRD analyses and the extraction of the crystalline fractions from the XRD data. The Department of Chemical Technology, section R&CE, of the Delft University of Technology is acknowledged for the use of their Raman microscope. The authors thank Niek van de Pers for the XRD analysis (Fig. 5). NOVEM is acknowledged for financial support.

[1] R. E. I. Schropp and M. Zeman, Amorphous and Microcrystalline Silicon Solar Cells (Kluwer, Dordrecht, 1998).
[2] L. Houben, M. Luysberg, P. Hapke, R. Carius, F. Finger, and H. Wagner, Philos. Mag. A **77**, 1447 (1998).
[3] D. L. Williamson, Mater. Res. Soc. Symp. Proc. **557**, 251 (1999).
[4] P. Roca i Cabarrocas and S. Hamma, Thin Solid Films **337**, 23 (1999).
[5] H. Richter, Z. P. Wang, and L. Ley, Solid State Commun. **39**, 625 (1981).
[6] R. Rizzoli, C. Summonte, J. Plá, E. Centurioni, G. Ruani, A. Desalvo, and F. Zignani, Thin Solid Films **383**, 7 (2001).
[7] Z. Iqbal, S. Vepřek, A. P. Webb, and P. Capezzuto, Solid State Commun. **37**, 993 (1981).
[8] I. H. Campbell and P. M. Fauchet, Solid State Commun. **58**, 739 (1986).
[9] H. Touir, J. Dixmier, K. Zellama, J. F. Morhange, and P. Elkaim, J. Non-Cryst. Solids **227**, 906 (1998).
[10] D. V. Tsu, B. S. Chao, and S. R. Ovshinski, Appl. Phys. Lett. **71**, 1317 (1997).
[11] T. Ishidate, K. Inoue, K. Tsuji, and S. Minomura, Solid State Commun. **42**, 197 (1982).
[12] W. M. M. Kessels, R. J. Severens, A. H. M. Smets, B. A. Korevaar, G. J. Adriaenssens, D. C. Schram, and M. C. M. van de Sanden, J. Appl. Phys. **89**, 2404 (2001).
[13] B. A. Korevaar, C. Smit, R. A. C. M. M. van Swaaij, A. H. M. Smets, W. M. M. Kessels, J. W. Metselaar, D. C. Schram, and M. C. M. van de Sanden, *Proceedings of the 16th European Photovoltaic Solar Energy Conference* (James & James Ltd. (Science Publishers), London, 2000), B119.
[14] H. P. Klug and L. E. Alexander, *X-ray Diffraction Procedures*, 2nd ed. (Wiley, New York, 1974).
[15] Z. Iqbal and S. Vepřek, J. Phys. C **15**, 377 (1982).
[16] R. Tsu, J. Gonzalez-Hernandez, S. S. Chao, S. C. Lee, and K. Tanaka, Appl. Phys. Lett. **40**, 534 (1982).
[17] A. T. Voutsas, M. K. Hatalis, J. Boyce, and A. Chiang, J. Appl. Phys. **78**, 6999 (1995).
[18] E. Bustarret, M. A. Hachicha, and M. Brunel, Appl. Phys. Lett. **52**, 1675 (1988).
[19] S. Vepřek, F. A. Sarot, and Z. Iqbal, Phys. Rev. B **36**, 3344 (1987).
[20] Since not all information is available, all Gaussian line profile parameters were free to vary and we included the data in the range 400 cm^{-1} to 550 cm^{-1} in the fitting procedure.
[21] The data range that is included in the fit procedure is not mentioned, so we took the range of 400 cm^{-1} to 550 cm^{-1} in the fitting procedure.
[22] C. Ossadnik, S. Vepřek, and I. Gregora, Thin Solid Films **337**, 148 (1999).